in eight-vertex systems will, however, have to await further synthetic and structural studies of related compounds.

Acknowledgment. We thank the National Science Foundation (Grant CHE-77-06793) and the University of Pennsylvania Materials Research Laboratory (Grant DMR-76-00678) for the support of this research.

Registry No. $4,5,7,8-(C_6H_5)_4-1,4,5,7,8-(\eta-C_5H_5)CoC_4B_3H_3$, 74964-99-1.

Supplementary Material Available: A listing of observed and calculated structure factors (17 pages). Ordering information is given on any current masthead page.

Contribution from the Department of Chemistry, Biochemistry and Biophysics, Massey University, Palmerston North, New Zealand,
the Chemistry Division, DSIR, Petone, New Zealand, and the Chemistry Department, Drexel University,
Philadelphia, Pennsylvania 19104

Small Molecule Analogues for the Specific Iron-Binding Site of Lactoferrin: A Single-Crystal X-ray Structure of Bis(methanol)bis[2-(5-methylpyrazol-3-yl)phenolato]iron(III) Nitrate–Methanol and Spectroscopic Studies on Iron(III) Phenolate Complexes

ERIC W. AINSCOUGH,*[1a] ANDREW M. BRODIE,*[1a] JEFFREY E. PLOWMAN,[1a] KEVIN L. BROWN,*[1b] ANTHONY W. ADDISON,[1c] and A. ROSS GAINSFORD[1b]

Received June 11, 1980

In an attempt to model the specific iron-binding site of the human milk protein, lactoferrin, a range of iron(III) phenolate complexes, embracing the chromophore types FeO_6 to $FeO_2N_2O'_2$ (where O represents a phenolate oxygen, N an aliphatic or aromatic nitrogen, and O′ a carboxylate oxygen or a methanolic oxygen) (see Figure 1 for the ligands used), has been studied to determine which types spectroscopically match diferric lactoferrin. In particular the factors that influence the energy of the oxygen $p_\pi \rightarrow d_\pi^*$ charge-transfer band have been investigated, and it is found that increasing the number of phenolate oxygens and imidazole nitrogens bound to iron(III) results in a hypsochromic shift, whereas increased binding strength results in a bathochromic shift. It has been found that EPR and Mössbauer spectra are insensitive to variations in ligand types and numbers. A single-crystal X-ray structure on one of the complexes, bis(methanol)bis[2-(5-methylpyrazol-3-yl)phenolato]iron(III) nitrate–methanol, $[Fe(IIIa)_2(MeOH)_2]NO_3\cdot MeOH$, has been determined by direct methods and refined by least-squares methods to a conventional R factor of 0.045. A total of 1451 reflections with $I > 3\sigma(I)$ were used. The dark purple needlelike crystals have space group $P2_1/n$, with $Z = 2$, and unit cell dimensions $a = 11.326$ (2) Å, $b = 7.384$ (1) Å, $c = 17.918$ (2) Å, and $\beta = 107.72$ (1)°. The iron atom lies on a center of symmetry and is required to be coplanar with the IIIa ligand donor atoms which are arranged in an all-trans arrangement. The Fe–O(phenolate) bond length is 1.888 (3) Å, and Fe–N is 2.068 (3) Å. The two methanol molecules are axially coordinated with Fe–O bond lengths of 2.094 (3) Å. They are hydrogen bonded to the lattice methanol, which is hydrogen bonded to ionic nitrate, which is further hydrogen bonded to the N–H proton of the pyrazolyl group. Collectively the data support the iron of diferric lactoferrin occupying a site of rhombic symmetry and bound to three tyrosyl and two cis histidyl residues, while the bicarbonate (or carbonate) ion, which is isoelectronic with the nitrate ion, may be hydrogen bonded to a coordinated aquo ligand.

Introduction

Lactoferrin occurs in high concentrations in human milk and also in other bodily secretions and intracellular components.[2-4] Its physiological role has yet to be defined with certainty, but, because of its ability to bind iron(III) tightly, it has been postulated to have a bacteriostatic function in depriving microorganisms of essential iron for their growth,[5] and a nutritional role has also been suggested.[6] Like the related proteins human serum transferrin and ovotransferrin, lactoferrin has a molecular weight of about 80 000 and specifically binds two high-spin iron(III) ions concomitantly with two bicarbonate ions.[2-4]

Recently we reported[7] that lactoferrin (Lf) forms complexes of the type M_2Lf (M = Cr(III), Mn(III), Co(III)) which, along with the known Fe_2Lf and Cu_2Lf, exhibit electronic absorption spectra similar to transferrin (Tf) and ovotransferrin analogues.[8-10] However, the exact nature and number of the groups involved in the binding of these metal ions have not been resolved. Spectrophotometric titrations and UV difference spectra have indicated that for all three iron-binding proteins three tyrosyl residues are involved[11-15] while other evidence suggests only two[10,16] per each iron atom. Binding of each iron to transferrin has been found to protect two histidines from ethoxyformylation, and the protein remains active.[17] One water molecule has also been found to be bound to each iron from NMR studies.[18] The precise involvement of bicarbonate, essential for the binding of iron,[19] is still uncertain. Studies indicate that transferrin has an essential arginine residue for each iron-binding center[20] which in its

---

(1) (a) Massey University. (b) Chemistry Division, DSIR. (c) Drexel University.

(2) Feeney, R. E.; Komatsu, S. S. *Struct. Bonding* (*Berlin*) **1966**, *1*, 149.

(3) Aisen, P. "Inorganic Biochemistry"; Eichorn, G. I., Ed.; Elsevier: Amsterdam, 1973; p 280.

(4) Bezkorovainy, A. *J. Dairy Sci.* **1977**, *60*, 1023.

(5) Bullen, J. J.; Rogers, H. J.; Griffiths, E. "Microbial Iron Metabolism"; Neilands, J. B., Ed.; Academic Press: New York, 1974; p 517.

(6) McMillan, J. A.; Landaw, S. A.; Oski, F. A. *Pediatrics* **1976**, *58*, 686.

(7) Ainscough, E. W.; Brodie, A. M.; Plowman, J. E. *Inorg. Chim. Acta* **1979**, *3*, 149.

(8) Aisen, P.; Aasa, R.; Redfield, A. G. *J. Biol. Chem.* **1969**, *244*, 4628.

(9) Tomimatsu, Y.; Kint, S.; Scherer, J. R. *Biochemistry* **1976**, *15*, 4918.

(10) Gaber, B. P.; Miskowski, V.; Spiro, T. G. *J. Am. Chem. Soc.* **1974**, *96*, 6868.

(11) Aisen, P.; Leibman, A. *Biochim. Biophys. Acta* **1972**, *257*, 314.

(12) Warner, R. G.; Weber, J. *J. Am. Chem. Soc.* **1953**, *75*, 5094.

(13) Teuwissen, B.; Masson, P. L.; Osinski, P.; Heremans, J. F. *Eur. J. Biochem.* **1972**, *31*, 239.

(14) Wishnia, A.; Weber, I.; Warner, R. G. *J. Am. Chem. Soc.* **1961**, *83*, 2071.

(15) Bezkorovainy, A.; Grohlich, D. *Biochim. Biophys. Acta* **1972**, *263*, 645.

(16) Phillips, J. L.; Azari, P. *Arch. Biochem. Biophys.* **1972**, *151*, 445.

(17) Rogers, T. B.; Gold, A.; Feeney, R. E. *Biochemistry* **1977**, *16*, 2299.

(18) Koenig, S. H.; Schillinger, W. E. *J. Biol. Chem.* **1969**, *244*, 6520.

(19) Price, E. M.; Gibson, J. F. *Biochem. Biophys. Res. Commun.* **1972**, *46*, 646.

0020-1669/80/1319-3655$01.00/0

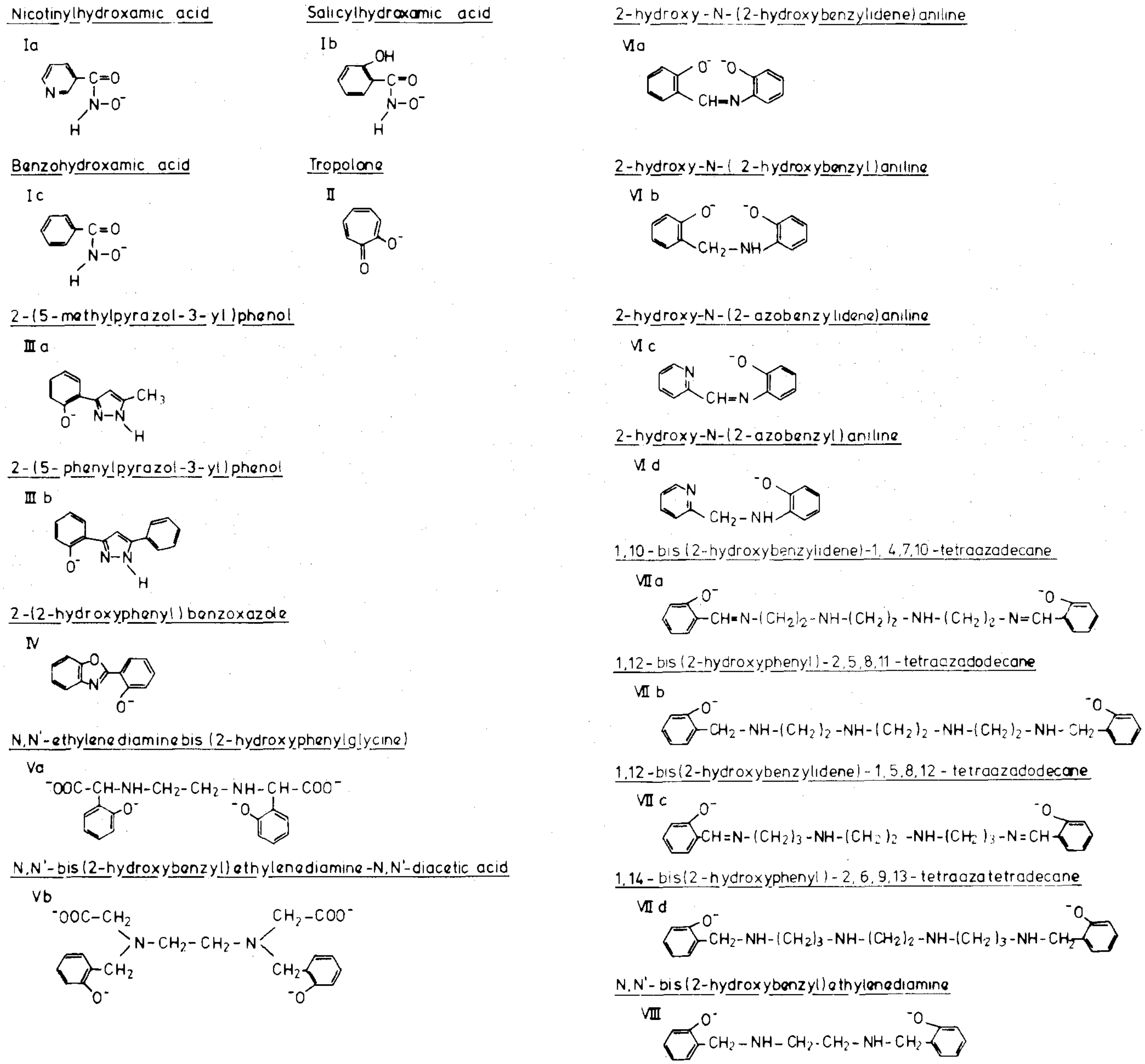

Figure 1. Structures and abbreviations of ligands used. The number and structure refer to the deprotonated ligand; the name refers to the corresponding acid form.

cation form may bind bicarbonate, and current opinion favors the bicarbonate bound to each iron as well in a so-called "interlocking site".[21-24]

Another approach in trying to resolve some of these uncertainties is to study appropriate small molecule compounds to find the best spectroscopic match. One study has been reported for iron transferrin, but this was limited to a single ligand study,[10] and so to obtain more extensive data we have studied a comprehensive range of model complexes with use of the ligands illustrated (with appropriate abbreviations) in Figure 1. These ligands allowed us to study spectroscopically a series of complexes embracing the donor types FeO_6, FeO_4N_2, FeO_3N_3, FeO_2N_4, and $FeO_2N_2O'_2$ (O represents a phenolate oxygen, O' a carboxylate oxygen, and N a nitrogen donor ligand) and hence to determine their usefulness as models. To clarify the electronic spectra we have selected ligands which are essentially colorless in the anionic form. To mimic the tyrosine moiety we have used substituted hydroxyphenyl derivatives wherever possible; however, for the FeO_6 type data obtained for catecholate and hydroxamate complexes were used as similar phenolate complexes are not known. Ideally, monodentate (nonconjugated) tyrosine and histidyl systems should be considered, but these are, unfortunately, not easy to isolate or are unknown, so systems containing bidentate, tridentate or hexadentate ligands with phenolate oxygens and aromatic and/or aliphatic nitrogens (which result in isolatible complexes) have been prepared and factors that influence the peak position and intensity of the charge-transfer band in the visible region studied. EPR and Mössbauer spectroscopies of the systems were also considered, to evaluate their sensitivity to changes in the ferric ion environment. From these studies conclusions were drawn about the nature of the iron binding in lactoferrin.

---

(20) Rogers, T. B.; Børresen, T.; Feeney, R. E. *Biochemistry* **1978**, *17*, 1105.
(21) Harris, D. C.; Aisen, P. *Fed. Proc., Fed. Am. Soc. Exp. Biol.* **1974**, *33*, 1503.
(22) Aisen, P.; Pinkowitz, R. A.; Leibman, A. *Ann. N.Y. Acad. Sci.* **1973**, *222*, 337.
(23) Schlabach, M. R.; Bates, G. W. *J. Biol. Chem.* **1975**, *250*, 2182.
(24) Najaran, R. C.; Harris, D. C.; Aisen, P. *J. Biol. Chem.* **1978**, *253*, 38.

Experimental Section

Synthesis of the Ligands. Figure 1 names the ligands and gives the abbreviations used. Ia, Ic, II, and IV were obtained from the Aldrich Chemical Co., Ib was obtained from the National Biochemical Corp., Vb was obtained from the Sigma Chemical Co., and imidazole and *N*-methylimidazole were obtained from BDH Laboratories. IIIa and IIIb were prepared by the condensation of hydrazine with salicyloylacetone or *o*-hydroxydibenzoylmethane (from Frinton Laboratories), respectively, and Vb was prepared by Coordination Chemistry Consultants (Texas A&M University). Ligands VIa, VIc, and salen (bis(salicylaldehyde)-*N*,*N'*-ethylenediamine) were made by adding 10 mmol of the appropriate aldehyde to 10 mmol of the appropriate amine in EtOH, warming gently, and stirring for $^1/_2$ h. If no precipitate appeared, the solution was taken to dryness and the solid washed with ether and air-dried. VIII was prepared by reduction of salen with $NaBH_4$ in methanol.

Preparation of $[Fe(Ia)_3]\cdot 6H_2O$, $[Fe(Ib)_3]\cdot 4^1/_2H_2O$, $[Fe(Ic)_3]\cdot 1^1/_2H_2O$, and $[Fe(II)_3]$. The first three were prepared by the method of Epstein and Straub[25] while the latter was prepared according to the method of Cook et al.[26]

Preparation of $[Fe(IIIa)_3]\cdot 1^1/_2H_2O$. Ligand IIIa (0.52 g, 3 mmol) and NaOH (0.12 g, 3 mmol) were dissolved in approximately 30 cm^3 of hot methanol. To the filtered, cooled solution was added $Fe(NO_3)_3\cdot 9H_2O$ (0.404 g, 1 mmol) in 20 cm^3 of methanol, whereupon a fine blood red precipitate formed. This was filtered and washed first with methanol/diethyl ether and then diethyl ether and air-dried. The molecular weight of this was determined to be 604 (theoretical value is 575). Anal. Calcd for $FeC_{30}H_{27}O_3N_6\cdot 1^1/_2H_2O$: C, 59.8; H, 5.0; N, 14.0. Found: C, 59.5; H, 4.7; N, 13.4. The conductivity in acetone is 0 Ω^{-1} mol^{-1} cm^2. The magnetic moment is 5.90 μ_B.

Preparation of $[Fe(IIIa)_2(MeOH)_2]NO_3\cdot 2H_2O$. Ligand IIIa (0.35 g, 2 mmol) and NaOH (0.08 g, 2 mmol) were dissolved in approximately 30 cm^3 of hot methanol, and the solution was filtered after cooling. To this was added $Fe(NO_3)_3\cdot 9H_2O$ (0.404 g, 1 mmol) in 20 cm^3 of methanol. Initially, a red solution formed with precipitation of $[Fe(IIIa)_3]\cdot 1^1/_2H_2O$, but on addition of all the ferric nitrate, the solution turned purple and the precipitate redissolved. Within 5 min fine needle crystals appeared, and these were allowed to grow for a period of 2–4 h after which they were filtered off, washed with water, and air-dried. Anal. Calcd for $FeC_{24}H_{13}O_3N_4NO_3\cdot 2H_2O$: C, 46.8; H, 5.4; N, 12.4. Found: C, 46.7; H, 4.8; N, 12.8. The conductivity in EtOH is 35.8 Ω^{-1} mol^{-1} cm^2 and in nitrobenzene is 0.11 Ω^{-1} mol^{-1} cm^2. The magnetic moment is 5.79 μ_B.

Preparation of $[Fe(IIIa)_2(Im)_2]NO_3\cdot {}^1/_2H_2O$. To a hot solution of 0.188 g (0.333 mmol) of $[Fe(IIIa)_2(MeOH)_2]NO_3\cdot 2H_2O$ in ethanol was added a large (~10-fold) excess of imidazole until the λ_{max} no longer shifted to shorter wavelength. The solution was left to stand at 4 °C for 3 days after which the resulting dark red crystals were filtered and then washed with ethanol and ether. Anal. Calcd for $FeC_{26}H_{17}O_2N_8\cdot NO_3\cdot {}^1/_2H_2O$: C, 51.9; H, 4.8; N, 21.0. Found: C, 52.0; H, 4.5; N, 20.7.

Preparation of $[Fe(IIIb)_3]\cdot 4H_2O$. Ligand IIIb (0.708 g, 3 mmol) and NaOH (0.12 g, 3 mmol) were dissolved in approximately 30 cm^3 of hot methanol, and the solution was filtered after cooling. Upon the addition of $Fe(NO_3)_3\cdot 9H_2O$ (0.40 g, 1 mmol) in 20 cm^3 of methanol, a deep red solution formed. A deep red crystalline material was obtained after standing for $1^1/_2$ h. It was filtered, washed with water, ethanol, and diethyl ether, and air-dried. Further crops were obtained upon standing for 2 days and, after filtration, by the addition of water. Anal. Calcd for $FeC_{45}H_{33}O_3N_6\cdot 4H_2O$: C, 64.8; H, 5.0; N, 10.1. Found: C, 64.3; H, 4.4; N, 9.8. The conductivity in EtOH is 1.35 Ω^{-1} mol^{-1} cm^2. The magnetic moment is 6.13 μ_B.

Preparation of $[Fe(IV)_3]\cdot 1^1/_2H_2O$. Sodium metal (0.138 g, 6 mmol) was added to a slurry of ligand IV in 30 cm^3 of ethanol. As the sodium dissolved and the ligand converted to its anodic form, a red solution that fluoresced was produced. To the filtered solution was added $Fe(NO_3)_3\cdot 9H_2O$ (0.808 g, 2 mmol) in 20 cm^3 of ethanol. The resulting red precipitate was filtered, washed with water and then ethanol, and air-dried. Anal. Calcd for $FeC_{39}H_{24}O_6N_3\cdot 1^1/_2H_2O$: C, 65.7; H, 3.8; N, 5.9. Found: C, 65.7; H, 3.7; N, 5.8. The magnetic moment was 4.25 μ_B at room temperature.

Preparation of $K[Fe(Vb)]\cdot 2H_2O$. This was prepared by using the method of Gaber et al.[10] for the analogous Va complex. Equimolar quantities of Vb, freshly precipitated hydrated ferric oxide, and $KHCO_3$ were stirred in a 3:1 water/methanol mixture for 3 days. The solution was filtered and evaporated on a rotary evaporator and the resulting precipitate extracted into ethanol. Crystals which appeared when the volume was reduced were filtered and washed with diethyl ether. A second crop was obtained upon the addition of ether. Anal. Calcd for $KFeC_{20}H_{40}O_4N_2\cdot 2H_2O$: C, 46.6; H, 4.7; N, 5.4. Found: C, 46.2; H, 5.0; N, 5.3. The magnetic moment was 5.76 μ_B at room temperature, and the conductivity in EtOH was 76.8 Ω^{-1} mol^{-1} cm^2.

Preparation of $K[Fe(VIa)_2]\cdot 2H_2O$. To VIa (0.53 g, 2.48 mmol) and KOH (0.28 g, 5 mmol) dissolved in 35 cm^3 of warm ethanol was added $FeCl_3$ (0.20 g, 1.25 mmol) in 10 cm^3 of ethanol. The mixture was heated for 5 min and left to stand for 1 h. The solution was filtered to remove KCl and then reduced to below half-volume, and ether was added. The solution was cooled overnight, and black crystals of the product were collected and washed with an ethanol/ether (1:1 v/v) mixture and then diethyl ether. The product was recrystallized from a methanol/diethyl ether mixture. Anal. Calcd for $KFeC_{26}H_{18}O_4N_2\cdot 2H_2O$: C, 56.4; H, 3.9; N, 5.1. Found: C, 57.0; H, 4.1; N, 5.4. The magnetic moment (μ_β) was 5.98 μ_B at room temperature, and the conductivity in acetone was 93 Ω^{-1} mol^{-1} cm^2.

Preparation of $[Fe(VIIb)]PF_6$. $[Fe(VIIa)]NO_3\cdot 1^1/_2H_2O$ was prepared according to Tweedle and Wilson.[27] One gram of this compound was dissolved in water and 0.55 g of $NaBH_4$ slowly added. The solution changed to a wine red color. It was filtered, and KPF_6, dissolved in water, was added which resulted in the precipitation of the product. It was collected and washed thoroughly with water. Anal. Calcd for $FeC_{20}H_{28}O_2N_4PF_6$: C, 43.1; H, 5.0; N, 10.0. Found: C, 43.3; H, 5.0; N, 10.0. The magnetic moment is 5.90 μ_B.

Preparation of $[Fe(VIIc)]PF_6$. This was prepared in a similar manner to the literature preparation of $[Fe(VIIa)]PF_6$,[27] except at the extraction stage, where 900 cm^3 of water was used. The product was recrystallized from 30 cm^3 of an acetone/water mixture of (7:3 v/v). Anal. Calcd for $FeC_{22}H_{28}O_2N_4PF_6$: C, 45.6; H, 4.8; N, 9.6. Found: C, 45.8; H, 4.7; N, 9.4. The conductivity in MeOH is 89 Ω^{-1} mol^{-1} cm^2. The magnetic moment is 2.02 μ_B.

Preparation of $[Fe(VIIc)]I_3$. To 0.29 g of $[Fe(VIIc)]PF_6$ dissolved in 50 cm^3 of a methanol/acetone mixture (1:1 v/v) was added 0.4 g of I_2. After removal of the solvent mixture to below half-volume on a rotary evaporator, blackish crystals of the product precipitated. These were collected and washed with diethyl ether. Anal. Calcd for $FeC_{22}H_{28}O_2N_4I_3$: C, 32.3; H, 3.4; N, 6.9. Found: C, 32.3; H, 3.4; N, 6.9. The conductivity in MeOH is 93 Ω^{-1} mol^{-1} cm^2. The magnetic moment is 1.92 μ_B.

Preparation of $[Fe(VIc)_2]PF_6\cdot H_2O$. To VIc (0.39 g, 2 mmol) and KOH (0.112 g) dissolved in warm methanol (30 cm^3) was added $FeCl_3$ (0.16 g, 1 mmol) dissolved in 10 cm^3 of methanol. The mixture was heated for 10 min and 5 cm^3 of dimethoxypropane added. After cooling (1 h) the solution was filtered (to remove KCl) and the volume reduced to about 15 cm^3. NH_4PF_6 (2 mmol) dissolved in methanol was added, and the resulting precipitate was collected and washed with cold methanol and diethyl ether. Anal. Calcd for $FeC_{24}H_{18}N_4O_2PF_6\cdot H_2O$: C, 47.0; H, 3.3; N, 9.1. Found: C, 47.0; H, 3.6; N, 9.4. The conductivity in acetone was 110 Ω^{-1} mol^{-1} cm^2. The magnetic moment was 4.86 μ_B.

Interaction of Fe(III) Salts with VIb, VId, VIId, and VIII. In no case was the complex isolated as a solid from the solution, but some of these solutions were used for further studies with bases. The iron complexes containing the ligands VIb, VId, and VIId were formed by the reduction in aqueous solution of the complexes $K[Fe(VIa)_2]\cdot 2H_2O$, $[Fe(VIc)_2]PF_6$, and $[Fe(VIIc)]PF_6$, respectively, with $NaBH_4$, while ligand VIII was added to a methanol solution of anhydrous $Fe(ClO_4)_3$ to give a purple solution to the iron complex. The solutions were purged with dinitrogen.

X-ray Crystallography

The crystals of $[Fe(IIIa)_2(MeOH)_2]NO_3\cdot MeOH$ were long, dark purple needles (discussed below), which became amorphous to X-rays about 4–5 h after removal from the mother liquor. Consequently, crystals for X-ray diffraction were removed from the mother liquor and immediately encased in fast-setting epoxy resin. After considerable

---

[25] Epstein, L. M.; Straub, D. K. *Inorg. Chem.* **1969**, *8*, 453.

[26] Cook, J. W.; Gibb, A. R.; Raphiel, R. A.; Sommerville, A. R. *J. Chem. Soc.* **1951**, 503.

[27] Tweedle, M. F.; Wilson, L .J. *J. Am. Chem. Soc.* **1976**, *98*, 4824.

difficulty, a crystal suitable for analysis was found. (ω scans of several intense low-angle reflections had peak widths at half-height of $\leq 0.15°$.)

Preliminary photography indicated monoclinic symmetry, and the systematic absences $h0l$, $h + l = 2n + 1$, and $0k0$, $k = 2n + 1$, confirmed the space group $P2_1/n$. Lattice constants, and the orientation matrix used for data collection, were obtained[28] from the least-squares refinement of diffractometer settings for 12 intense reflections having $22° < \theta(\text{Cu K}\alpha) < 27°$. The unit cell dimensions are $a = 11.326$ (2) Å, $b = 7.384$ (1) Å, $c = 17.918$ (2) Å, and $\beta = 107.72$ (1)°, and there are two molecules/unit cell.

Data were collected by using a Hilger and Watts Y290 autodiffractometer and a $\theta/2\theta$ scan. As the stability of the crystal to X-rays was in some doubt, we resolved to collect the data as fast as possible. Consequently, we used Cu Kα radiation for greater intensity and a scan of 40 steps of 0.02°/step and a count time of 1.5 s/step. The local background was measured for 10 s at either end of the step scan by using the stationary counter/stationary crystal technique. A total of 2142 reflections for which $\theta(\text{Cu K}\alpha) \leq 57°$ were collected. The intensities of three standard reflections measured periodically throughout the data collection showed an essentially linear *increase* of around 11%. The reason for this increase is not clear; however one could propose that the very labile methanol molecules became more ordered when completely enclosed in the epoxy resin. The data were corrected for this rise in intensity, and the 1451 unique reflections for which $I > 3\sigma(I)$ were used in the subsequent structure solution and least-squares refinement. Absorption corrections were not applied due to the unknown absorption of the epoxy resin and the difficulty in describing the irregular crystals.

Structure Solution and Refinement

The structure was solved by symbolic addition, after unsuccessful attempts with MULTAN.[29] The resulting E map gave positions for 17 of the 22 nonhydrogen atoms. The remaining nonhydrogen atoms were located by the normal succession of least-squares refinement and difference Fourier maps.[30] All hydrogen atoms were clearly recognizable in a difference Fourier synthesis. The structure was refined to convergence with use of anisotropic thermal parameters for all nonhydrogen atoms and by refining only the positional parameters of the hydrogen atoms ($U_H = 0.08$ Å^2). The final discrepancy indices were

$$R_1 = \sum||F_o| - |F_c||/\sum|F_o| = 0.045$$

$$R_2 = [\sum w(|F_o| - |F_c|)^2/\sum w|F_o|^2]^{1/2} = 0.043$$

The function minimized during least-squares refinement was $\sum w(|F_o| - |F_c|)^2$ where $w = 1/(\sigma(F))^2$, and an uncertainty factor of $p = 0.05$[31] was used in the calculation of the weights. During the final refinement cycle, no parameter moved by more than 0.6 of its esd. A final difference Fourier synthesis showed no peaks of chemical significance, the highest peak being 0.2 e/Å^3. A listing of the observed and calculated structure factors is available as supplementary material.

Instrumentation

IR spectra were recorded on a Beckman IR20 spectrophotometer, and electronic spectra were recorded on a Shimadzu MPS 5000 spectrophotometer. ESR measurements were made at −196 °C on a Varian E104A X-band spectrometer or at −160 °C by using a Varian E-257 variable-temperature accessory. Spectral g values were calibrated with a DPPH standard. Conductivity measurements were made by using a Philips PR 9500 and 9510 conductivity meter and cell at 10^{-3} M. Molecular weights were determined by the vapor pressure method on the Hitachi Perkin-Elmer Molecular Weight Apparatus 115. Magnetic susceptibilities were determined at Victoria University by the Faraday method using $Hg[Co(NCS)_4]$ as the calibrant. Pascal constants were used to correct for water, ligand, and anion diamagnetism. Mössbauer spectra were collected and analyzed at the Chemistry Division, DSIR. Analytical results are by Professor A. D. Campbell at Otago University.

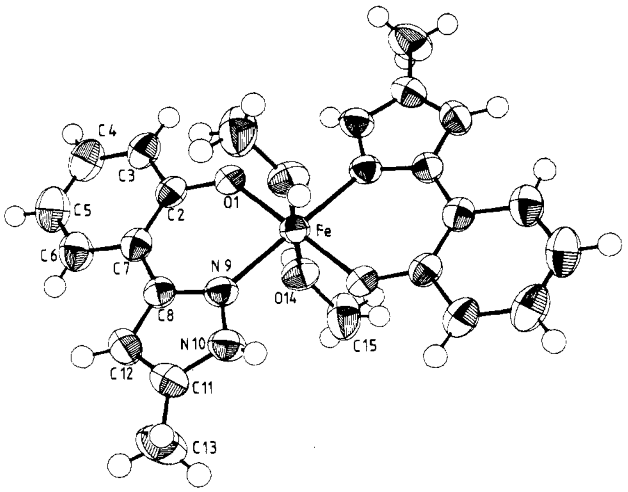

Figure 2. View of $[Fe(IIIa)_2(MeOH)_2]NO_3{\cdot}MeOH$ showing the atom numbering scheme.

Results and Discussion

Synthesis of Iron(III) Complexes. Some of the complexes were prepared according to published literature methods, while some were new (see Experimental Section). $[Fe(IIIa)_2(MeOH)_2]NO_3{\cdot}MeOH$ crystallized from a 1:2:2 mixture of $Fe(NO_3)_3{\cdot}9H_2O$/IIIa/NaOH in methanol as long purple needles which remained stable in air for 5 h but lost the lattice MeOH after several days and gained two lattice waters, the new formulation being $[Fe(IIIa)_2(MeOH)_2]NO_3{\cdot}2H_2O$. The addition of Me_2S and Me_2PhPO to a methanol solution of the above complex results in no change of λ_{max} at 563 nm (Table IV). Large additions of Me_2PhPO decrease the intensity of the charge-transfer band, suggesting the replacement of IIIa. Shifts of λ_{max} were noted with Me_2SO, tribenzylamine, and imidazole (Im), and for the latter base, $[Fe(IIIa)_2(Im)_2]NO_3{\cdot}{}^1/_2H_2O$ was isolated. When the ratio of Fe(III):IIIa was 1:3, $[Fe(IIIa)_3]{\cdot}1^1/_2H_2O$ was isolated; however when the Fe(III):IIIa ratio was 1:1, a deep blue solution was obtained of a 1:1 complex, but no solid was isolated. Interestingly, attempts to prepare the $[Fe(IIIb)_2(MeOH)_2]^+$ ion resulted in a mixture of this compound and $[Fe(IIIb)_3]{\cdot}4H_2O$ as shown by the visible absorption spectra. With ligand VIII, no Fe(III) complex could be isolated, but the solutions were used for spectroscopic studies with bases.

When ligand VIIa was complexed to iron, the addition of $NaBH_4$ resulted in a reduction of the two imine bonds, this being verified by the IR spectrum of the product, $[Fe(VIIb)]PF_6$, which showed two ν(N–H) absorption bands at about 3300 cm^{-1} compared with one for the parent compound, and the disappearance of the ν(C=N) absorption at 1620 cm^{-1} for the parent compound. It was not possible to isolate, in pure form, similar products from the reduction of $K[Fe(VIa)_2]{\cdot}2H_2O$ and $[Fe(VIc)_2]PF_6{\cdot}H_2O$ with $NaBH_4$. Indeed their solutions were unstable toward aerial oxidation; hence spectra data were recorded immediately (in the presence of a small excess of $NaBH_4$). A large excess of $NaBH_4$ resulted in the formation of Fe(II) and a loss of color.

Molecular Structure of Bis(methanol)bis[2-(5-methylpyrazol-3-yl)phenolato]iron(III) Nitrate–Methanol. The final positional and thermal parameters are listed in Table I. The structure of the iron and ligand moieties is shown in Figure 2. Bond lengths and angles are given in Table II.

The iron atom is coordinated to two bidentate IIIa anions and two methanol molecules. As well, there is one occluded methanol molecule and one nitrate group present in the

---

(28) Busing, W. R.; Levy, H. A. *Acta Crystallogr.* **1957**, *10*, 180.

(29) Main, P.; Lessinger, L.; Woolfson, M. M.; Germain, G.; Declercq, J.-P. MULTAN 77, a system of computer programs for the automatic solution of crystal structures, 1977.

(30) Local programs were used for data reduction; otherwise the SHELX 76 program by G. M. Sheldrick was used.

(31) Corfield, P. W. R.; Doedens, R. J. Ibers, J. A. *Inorg. Chem.* **1967**, *6*, 197.

Table I. Positional ($\times 10^4$) and Anisotropic Thermal[a] ($\times 10^3$) Parameters for the Nonhydrogen Atoms of Bis(methanol)bis[2-(5-methylpyrazol-3-yl)phenolato]iron(III) Nitrate–Methanol and Hydrogen Atom Positional Parameters[b] ($\times 10^3$)

atom	*x*	*y*	*z*	U_{11}	U_{22}	U_{33}	U_{23}	U_{13}	U_{12}
Fe	5000	5000	5000	43 (1)	39 (1)	44 (1)	1 (1)	16 (1)	3 (1)
O1	5908 (3)	4858 (3)	4276 (2)	53 (2)	57 (2)	47 (2)	2 (1)	22 (1)	11 (1)
C2	5821 (4)	5697 (5)	3603 (2)	51 (2)	42 (2)	46 (2)	−9 (2)	16 (2)	−6 (2)
C3	6824 (4)	5596 (6)	3301 (3)	55 (3)	70 (3)	55 (3)	−8 (2)	25 (2)	−8 (2)
C4	6788 (5)	6444 (7)	2612 (3)	71 (3)	88 (4)	66 (3)	−7 (3)	38 (3)	−21 (3)
C5	5767 (6)	7403 (8)	2197 (3)	88 (4)	89 (4)	63 (3)	12 (3)	36 (3)	−18 (3)
C6	4763 (5)	7515 (6)	2471 (3)	75 (3)	66 (3)	58 (3)	9 (2)	26 (3)	−6 (3)
C7	4759 (4)	6667 (5)	3176 (2)	59 (3)	42 (2)	47 (2)	−4 (2)	19 (2)	−7 (2)
C8	3637 (4)	6782 (5)	3418 (2)	52 (2)	36 (2)	43 (2)	−4 (2)	12 (2)	−2 (2)
N9	3585 (3)	6134 (4)	4105 (2)	43 (2)	47 (2)	52 (2)	2 (2)	19 (2)	4 (2)
N10	2414 (3)	6455 (5)	4121 (2)	48 (2)	54 (2)	62 (3)	6 (2)	19 (2)	9 (2)
C11	1729 (4)	7273 (6)	3473 (3)	50 (3)	48 (3)	62 (3)	2 (2)	7 (2)	5 (2)
C12	2475 (4)	7514 (6)	3008 (2)	60 (3)	53 (3)	50 (3)	5 (2)	9 (2)	3 (2)
C13	417 (5)	7757 (10)	3348 (4)	53 (3)	99 (5)	105 (5)	22 (4)	18 (3)	22 (3)
O14	5768 (3)	7575 (4)	5309 (2)	63 (2)	47 (2)	71 (2)	−8 (1)	24 (2)	−5 (2)
C15	5683 (8)	8674 (7)	5933 (3)	155 (6)	55 (3)	58 (3)	−6 (3)	27 (4)	−13 (4)
O16	7783 (5)	8684 (6)	5021 (4)	96 (4)	102 (4)	157 (5)	−13 (4)	65 (4)	−18 (3)
C17	7863 (10)	9817 (11)	4430 (7)	130 (9)	105 (7)	183 (9)	−16 (6)	88 (8)	−3 (5)
N18	5000	0000	0000	56 (5)	94 (6)	61 (4)	−20 (4)	13 (3)	13 (6)
O19	4151 (9)	1072 (18)	9834 (5)	62 (5)	122 (8)	107 (6)	5 (5)	43 (5)	21 (7)
O20	4044 (10)	−493 (18)	166 (7)	65 (7)	124 (9)	153 (9)	−32 (7)	63 (7)	−7 (6)
O21	4869 (15)	−1542 (16)	182 (7)	130 (12)	102 (9)	164 (10)	39 (7)	38 (8)	8 (9)

atom	*x*	*y*	*z*	atom	*x*	*y*	*z*
H3	755 (5)	495 (6)	362 (3)	H133	9 (5)	841 (7)	290 (3)
H4	746 (5)	637 (6)	244 (3)	H14	636 (5)	780 (8)	525 (3)
H5	570 (4)	794 (7)	173 (3)	H151	564 (6)	959 (7)	582 (4)
H6	407 (4)	813 (7)	222 (3)	H152	546 (5)	804 (7)	631 (3)
H10	219 (5)	618 (8)	441 (3)	H153	648 (5)	684 (6)	639 (3)
H12	230 (4)	807 (7)	252 (3)	H16	816 (6)	805 (9)	516 (4)
H131	−5 (5)	668 (7)	328 (3)	H171	737 (5)	1063 (8)	439 (3)
H132	20 (5)	819 (7)	377 (3)	H172	866 (5)	998 (7)	448 (3)
				H173	731 (5)	926 (6)	383 (3)

[a] The U_{ij} values (in Å^2) correspond to the temperature factor expression $T = \exp[-2\pi^2(U_{11}h^2a^{*2} + \ldots + 2U_{12}hka^*b^* + \ldots)]$. [b] Named after the parent ion.

Table II. Bond Lengths (Å) and Angles (Deg) for Bis(methanol)bis[2-(5-methylpyrazol-3-yl)phenolato]iron(III) Nitrate–Methanol

Fe–O1	1.888 (3)	C8–N9	1.339 (4)
Fe–N9	2.068 (3)	C8–C12	1.406 (6)
Fe–O14	2.094 (3)	N9–N10	1.356 (5)
O1–C2	1.332 (4)	N10–C11	1.330 (5)
C2–C3	1.402 (5)	C11–C12	1.367 (6)
C2–C7	1.409 (5)	C11–C13	1.478 (7)
C3–C4	1.373 (6)	C15–O14	1.409 (6)
C4–C5	1.368 (7)	C17–O16	1.374 (11)
C5–C6	1.371 (7)	N18–O19	1.22 (1)
C6–C7	1.412 (6)	N18–O20	1.26 (1)
C7–C8	1.464 (5)	N18–O21	1.21 (1)
O1–Fe–O14	87.9 (1)	C2–C7–C8	122.9 (3)
N9–Fe–O14	89.9 (1)	C7–C8–C9	122.4 (3)
O1–Fe–N9	86.9 (1)	C7–C8–C12	128.8 (3)
Fe–O1–C2	133.6 (3)	N9–C8–C12	108.7 (3)
O1–C2–C3	118.6 (4)	Fe–N9–C8	128.1 (3)
O1–C2–C7	122.9 (4)	C8–N9–N10	105.9 (3)
C3–C2–C7	118.4 (4)	Fe–N9–N10	125.9 (3)
C2–C3–C4	121.2 (5)	N9–N10–C11	112.0 (3)
C3–C4–C5	120.9 (5)	N10–C11–C12	106.7 (4)
C4–C5–C6	119.5 (5)	N10–C11–C13	122.3 (5)
C5–C6–C7	121.5 (5)	C12–C11–C13	131.0 (4)
C6–C7–C2	118.4 (4)	C11–C12–C8	106.6 (4)
C6–C7–C8	118.6 (4)	Fe–O14–C15	127.6 (4)

crystallographic asymmetric unit. The position of the iron atom coincides with a crystallographic center of symmetry. The iron is bound to the phenolate oxygen and one (N9) of the imine nitrogen atoms as well as to the oxygen atom of the methanol molecule. These six atoms of the inner coordination sphere form a distorted octahedral environment for the iron atom. The iron–phenolate bond length (Fe–O1 = 1.888 (3) Å) is about the same as similar bonds in five-coordinated iron complexes[32,33] and Na[Fe(Va)]·4H_2O[34] but somewhat shorter than that in the $[Fe(catecholate)_3]^{3-}$ ion[35] (2.015 Å). The presence of six tightly bound oxygens and the negative charge for the latter complex may account for this lengthening. The Fe–N bond length is within the normally accepted values for iron–imine nitrogen interactions, and the iron–methanol oxygen bond length (Fe–O14 = 2.094 (3) Å) is not significantly different from similar Fe(III)–ethanol interactions[36] (2.113, 2.160 Å). Because of the crystallographic symmetry, the iron atom must lie exactly in the plane of all four-coordinated donor atoms of the two ligands IIIa. The angle between the planes of the two ring systems of the IIIa ligand is 7.2°, and the iron atom is 0.37 Å out of the plane of the phenolate ring but is nearly coplanar (Δ = 0.08 Å) with the heterocyclic ring.

As the nitrogen atom of the nitrate is positioned on a crystallographic center of symmetry, the ion must necessarily be disordered. In the preliminary photography, there was no indication of any long-range order in this group. The occluded methanol molecule is part of a hydrogen-bonding scheme involving the methanol molecule bound to the iron atom, the occluded methanol molecule, and the nitrate group (Figure 3, Table III). The "hydrogen-bonding" hydrogen atom of the bound methanol, H14, is hydrogen bonded to O16 of the

---

(32) Davies, J. E.; Gatehouse, B. M. *Acta Crystallogr., Sect. B* **1972**, *B28*, 3641.

(33) Coggon, P.; McPhail, A. T.; Mabbs, F. E.; McLachlan, V. N. *J. Chem. Soc. A* **1971**, 1014.

(34) Bailey, N. A.; Cummins, D.; McKenzie, D. E.; Worthington, J. M. *Inorg. Chim. Acta* **1976**, *18*, L13.

(35) Raymond, K. N.; Isied, S. S.; Brown, L. D.; Fronczek, F. R.; Nibert, J. H. *J. Am. Chem. Soc.* **1976**, *98*, 1767.

(36) Einstein, F. W. B.; Willis, A. C. *Inorg. Chem.* **1978**, *17*, 3040.

Table III. Hydrogen-Bonding Schemes[a]

O14-H14	0.72	H14---O16	1.90	O14---O16	2.62	O14-H14---O16	171.6
O16-H16	0.64	H16---O20	2.13	O16---O20	2.73	O16-H16---O20	156.7
O16-H16	0.64	H16---O21	2.22	O16---O21	2.78	O16-H16---O21	149.7
N10-H10	0.67	H10---O19	2.32	N10---O19	2.96	N10-H10---O19	157.4
N10-H10	0.67	H10---O20	2.17	N10---O20	2.78	N10-H10---O20	150.8

[a] Distances in Å; angles in deg.

Table IV. Electronic Spectra of the Ferric Complexes

compd	λ_{max},[a] nm		solvent
	visible bands	others	
Fe_2Lf[b]	465 (4140)	283 (115 800)	phosphate buffer
Fe_2Tf[c]	470 (4370)	280 (109 700)	Tris buffer
$[Fe(catecholate)_3]^{3-}$[d]	496 (4700)		H_2O
$[Fe(Ia)_3]\cdot 6H_2O$	433 (3430)	260 (sh)	EtOH
$[Fe(Ib)_3]\cdot 4^1/_2H_2O$	468	301	EtOH
$[Fe(Ic)_3]\cdot 1^1/_2H_2O$	444 (4470)	250 (sh)	EtOH
$[Fe(II)_3]$	427 (15 200), 510 (sh), 534 (sh)	270 (sh), 328 (31 700), 364 (17 300)	$CHCl_3$
$[Fe(IIIa)_3]\cdot 1^1/_2H_2O$	487 (3903)	304 (24 250)	$CHCl_3$
$[Fe(IIIa)_2(MeOH)_2]NO_3\cdot 2H_2O$	563 (4570)	305 (19 000)	EtOH
$[Fe(IIIa)_2(Im)_2]NO_3\cdot {}^1/_2H_2O$[e]	530		EtOH
$[Fe(IIIa)_2(X)_2]^{2+}$			
X = tribenzylamine	527		EtOH
$X = Me_2SO$	550		EtOH
$X = Me_2S$	no change		EtOH
$X = Me_2PhP{=}O$	no change		EtOH
$[Fe(IIIa)(MeOH)_4]^{2+}$	640		reflectance
$[Fe(IIIb)_3]\cdot 4H_2O$	501 (3870)	298 (39 900)	EtOH
$[Fe(IV)_3]\cdot 1^1/_2H_2O$	500 (sh, ~1500)	325 (35 170), 336 (35 280), 360 (sh)	$CHCl_3$
$[Fe(VIII)]^+$	540		MeOH
$[Fe(VIII)(Im)]^+$[e]	480		MeOH
$[Fe(VIII)(Im)_2]^+$[e]	490		MeOH
$[Fe(VIII)(N\text{-}MeIm)_2]^+$[f]	467		MeOH
$Na[Fe(Va)]\cdot 4H_2O$[g]	480 (4000), 910	282	H_2O
$K[Fe(Vb)]\cdot 2H_2O$	492 (3830)	277 (11 380), 318 (6300)	H_2O
$K[Fe(VIa)_2]\cdot 2H_2O$	403 (26 310), 470 (sh)	290 (30 840), 345 (sh)	MeOH
$K[Fe(VIb)_2]$	425		MeOH
$[Fe(VIc)_2]PF_6\cdot H_2O$	430 (sh)		acetone
$[Fe(VId)_2]PF_6$	465		MeOH
$[Fe(VIIa)]PF_6$	430 (3000), 490 (3600)	340 (9000)	acetone
$[Fe(VIIb)]PF_6$	507		MeOH
$[Fe(VIIc)]PF_6$	400 (sh), 575 (3000)	353 (6880)	MeOH
$[Fe(VIId)]PF_6$	509		MeOH
$[Fe(VIIc)]I_3$	410 (sh), 575 (3260)	256 (sh), 280 (sh), 359 (14 000)	MeOH

[a] Extinction coefficients ($L\ mol^{-1}\ cm^{-1}$) in brackets. [b] This work. [c] From ref 11. [d] From ref 44. [e] Im is imidazole. [f] *N*-MeIm is *N*-methylimidazole. [g] From ref 10.

occluded methanol molecule. The hydrogen atom of this molecule (H16) is in turn bonded to either O21 or O20 of the nitrate group, depending on which disordered form of the nitrate group is present. Also the proton (H10) bonded to N10 of ligand IIIa is hydrogen bonded to O19 or O20 of the nitrate group.

The magnetic moment as well as the EPR and Mössbauer spectra (see Tables V and VI) for this complex are in keeping with high-spin Fe(III). A band at 1360 cm^{-1} in the IR spectrum is consistent with a structure having ionic nitrate, while, in ethanol and nitrobenzene, conductivity measurements are interpreted in terms of only partial ionization of the nitrate (ion pairing is pronounced).

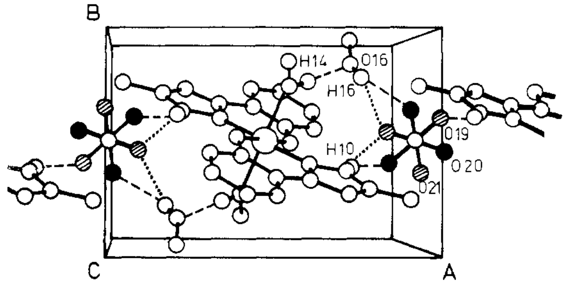

Figure 3. The hydrogen-bonding scheme in $[Fe(IIIa)_2(MeOH)_2]NO_3\cdot MeOH$. The oxygen atoms of one disordered form of the nitrate group are depicted as ●; the others as ⊘. The two hydrogen-bonding schemes between H16, H10, and the nitrate oxygens depend on which disordered form of the nitrate is present and are differentiated by dotted and dashed lines.

Electronic Spectra. The main feature of the electronic spectra of these compounds (Table IV) is the relatively intense charge-transfer (CT) band that gives rise to the reddish to purplish colors (at 420–530 nm) and which can be assigned to a transition from the p_π orbital on the phenolate oxygen to the half-filled d_π* orbitals on the ferric ion.[10] Such $p_\pi \rightarrow d_\pi$* transitions are intense, whereas d–d transitions are very weak and difficult to detect for Fe(III); e.g., for $Na[Fe(Va)]\cdot 4H_2O$ a weak shoulder at 900 nm, observed at room temperature and −196 °C, is of the latter type (Table IV). For the $[Fe(Va)]^-$ ion, a second CT band occurs at 315 nm and has been assigned as a $p_\pi \rightarrow d_\sigma$* type.[10] This band is poorly resolved in diiron transferrin[10] and Fe_2Lf (this work), and though discrete bands are seen at this wavelength with complexes of IIIa, IIIb, and IV, in the other complexes it is not seen. The high intensity of the CT bands is probably due to mixing with low-lying phenyl $\pi \rightarrow \pi$* transitions. Where these are absent, as in $[Fe(EDTA)(OH)]^{2-}$, no CT band is allowed.[37]

Table V. Electron Spin Resonance Spectra of the Ferric Complexes

compd	g values[a] (at −196 °C)	solvent
Fe_2Lf[b]	8.84, 4.39, 4.29, 4.15	phosphate buffer
Fe_2Tf[c]	9.18, 4.42, 4.16, 4.08	0.1 M KCl soln
$[Fe(Ia)_3]\cdot 6H_2O$	10.01, 4.15	EtOH
$[Fe(Ib)_3]\cdot 4^1/_2H_2O$	10.26, 4.42	EtOH
$[Fe(Ic)_3]\cdot 1^1/_2H_2O$	9.68, 4.36	EtOH
$[Fe(II)_3]$	8.11, 4.42	$CHCl_3$
$[Fe(IIIa)_3]\cdot 1^1/_2H_2O$	8.50, 4.23	acetone
$[Fe(IIIa)_2(MeOH)_2]NO_3\cdot 2H_2O$	7.33, 4.26	acetone
$[Fe(IIIa)_2(Im)_2]NO_3\cdot {}^1/_2H_2O$	8.07, 6.59, 4.28	DMF
$[Fe(IIIb)_3]\cdot 4H_2O$	8.28, 4.26	acetone
$[Fe(IV)_3]\cdot 1^1/_2H_2O$	7.88, 5.21, 4.18, 2.78	acetone
$[Fe(VIII)]^+$	9.63, 6.09, 4.25, 2.06	MeOH
$[Fe(VIII)(Im)]^+$	9.49, 4.25, 2.48, 2.01, 1.59	MeOH
$[Fe(VIII)(Im)_2]^+$	9.63, 4.25, 2.02	MeOH
$[Fe(VIII)(N\text{-}MeIm)_2]^+$	8.32, 4.24	MeOH
$Na[Fe(Va)]\cdot 4H_2O$	4.47	H_2O
$K[Fe(Vb)]\cdot 2H_2O$	4.26	EtOH
$K[Fe(VIa)_2]\cdot 2H_2O$	8.72, 4.24	MeOH
$K[Fe(VIb)_2]$	8.76, 4.18	MeOH
$[Fe(VIc)_2]PF_6\cdot H_2O$	2.18, 2.05, 1.94	MeOH
$[Fe(VId)_2]PF_6$	8.59, 4.21	MeOH
$[Fe(VIIa)]PF_6$	2.19, 2.13, 1.95	acetone
$[Fe(VIIb)]PF_6$	6.14, 4.78, 1.94	MeOH
$[Fe(VIIc)]PF_6$	2.34, 2.12, 1.95	acetone
$[Fe(VIId)]PF_6$	6.72, 4.12, 1.93	MeOH
$[Fe(VIIc)]I_3$	2.33, 2.13, 1.95	acetone

[a] At −196 °C. [b] This work and reference 11. [c] From reference 11.

Table VI. Mössbauer Spectral Data for Ferric Complexes at Room Temperature

compd	δ_{Fe},[a] mm/s	ΔEq, mm/s
Fe_2Lf[b]	0.39	
Fe_2Tf[c]	0.38	0.75
HCO_3^--free iron transferrin[d]	0.47	0.72
ferric hydroxide gel[d]	0.46	0.75
$Fe^{3+}alb$[d,e]	0.47	0.74
$[Fe(Ia)_3]\cdot 6H_2O$[f] (1)	0.41	0.92
(2)	0.02	
$[Fe(Ib)_3]\cdot 4^1/_2H_2O$[f]	0.50	1.01
$[Fe(Ic)_3]\cdot 1^1/_2H_2O$[f] (1)	0.48	0.68
(2)	0.02	
$[Fe(II)_3]$ (1)	0.53	0.56
(2)	−0.04	
$[Fe(IIIa)_3]\cdot 1^1/_2H_2O$	0.38	0.72
$[Fe(IIIa)_2(MeOH)_2]NO_3\cdot 2H_2O$	0.41	1.05
$[Fe(IIIb)_3]\cdot 4H_2O$	0.39	0.76
$[Fe(IV)_3]\cdot 1^1/_2H_2O$	0.34	1.21
$Na[Fe(Va)]\cdot 4H_2O$	0.37	0.77
$K[Fe(Vb)]\cdot 2H_2O$	0.38	0.75

[a] With respect to iron metal; the error in the determination of δ_{Fe} and ΔEq is ±0.03 mm/s. [b] From ref 45. [c] From ref 42. [d] From ref 43. [e] alb = albumin. [f] Previously reported in ref 25.

In any attempt to mimic the CT characteristics of Fe_2Lf (λ_{max} 465 nm, ϵ 2070 L mol^{-1} cm^{-1}/Fe(III) ion) it is important to recognize that the following factors will influence the intensity and position of the band: (1) the polydentate nature of some of the ligands as compared with the bidentate and tridentate character of others, (2) the charge on the ligand, (3) the nature of the N atoms (e.g., whether aliphatic or aromatic), (4) the stereochemistry of the ferric ion (e.g., for the FeO_3N_3 systems whether the *mer* or *fac* isomer exists and for FeO_2N_4 systems whether cis or trans isomers are present), (5) the actual number of phenolate and nitrogen donor atoms, (6) the basicity of the phenolate ligands present, and (7) the nature of the solvent in which the spectra are recorded. It is conceivable that particular combinations of the above factors will allow one to mimic the natural protein even though the numbers of phenolates and nitrogen atoms are different in each model; however a systematic study should limit the possibilities.

Ideally, it would be more suitable if monodentate phenoxides and imidazoles were studied, but as their iron solution chemistry is not well advanced, nor extensive, we have had to resort to ligand systems that gave well-defined compounds in solution and solid state. We have chosen quite a range of ligands to cover the structural types FeO_6 to $FeO_2N_2O'_2$. (See Figure 1.)

FeO_6 Types. Ligands Ia, Ib, Ic, and II give this type, and their CT bands lie in the range 430–500 nm (Table IV) making them similar to Fe_2Lf. Generally these bands are higher in energy than the bands in complexes of the type FeO_3N_3, indicating that the second oxygen in the ligand raises the electron density on iron to a greater extent than nitrogen; hence the CT interaction becomes less favorable. However, the spectrum of $[Fe(II)_3]$ is more complex than the others in this series because the anion of ligand II is already red.

FeO_4N_2, FeO_3N_3, and Related Types. In the series of complexes with ligand IIIa there is an increase in the energy of the charge-transfer band from $[Fe(IIIa)(MeOH)_4]^{2+}$ to $[Fe(IIIa)_2(MeOH)_2]^+$ and $[Fe(IIIa)_3]$, while the only FeO_4N_2 complex ion $[Fe(VIb)_2]^-$ (prepared in situ) absorbs at the highest energy (Table IV). This trend is consistent with the idea that complexation of the ferric ion by successive phenolate groups produces a blue shift in the visible absorption maximum by about 2000 cm^{-1}/phenolate group.[38,39] This interaction is expected to destabilize the metal d_π* orbitals. The CT transition moves from 487 nm for $[Fe(IIIa)_3]\cdot 1^1/_2H_2O$ to 510 nm for $[Fe(IIIb)_3]\cdot 4H_2O$, a move consistent with the fact that increasing conjugation of the ligand (e.g., with a phenyl substituent) reduces the p_π–p_π* energy gap. The complex $[Fe(IV)_3]\cdot 1^1/_2H_2O$ has a similar CT transition.

Addition of bases such as imidazole or tribenzylamine to $[Fe(IIIa)_2(MeOH)_2]NO_3\cdot 2H_2O$ shifts the absorbance maximum to higher energy though the shift is not as great as when similar bases are added to the $[Fe(VIII)]^+$ ion (Table IV). For the former case the phenolato groups are coordinated trans to each other and the imidazoles are trans, while for $[Fe(VIII)]^+$, the phenolates are likely to be cis to each other[40] and the imidazoles trans.

Previous workers have cited a trend in the extinction coefficients of an increase of 2000 L mol^{-1} cm^{-1}/phenolate group.[10] While $[Fe(IIIa)_2(MeOH)_2]NO_3\cdot 2H_2O$ has an extinction coefficient of 4570 L mol^{-1} cm^{-1}, $[Fe(IIIa)_3]\cdot 1^1/_2H_2O$ has a value of 3903 L mol^{-1} cm^{-1} and $[Fe(IIIb)_3]\cdot 4H_2O$ has a value of 3870 L mol^{-1} cm^{-1}, suggesting that a ceiling is reached after two phenolates are bound.

FeO_2N_4 and $FeO_2N_2O'_2$ Types. From models a cis arrangement of phenolates in $[Fe(VId)_2]PF_6$ is probable. The absorbance maximum for this compound is similar to that of the other cis FeO_2N_4 system, $[Fe(VIII)(N\text{-}MeIm)_2]^+$. Changing from the tridentate ligand VId to the hexadentate ligands VIIb and VIId (where the overall charge of the complexes remains the same) causes a shift in the CT band to

---

(37) Schugar, H. J.; Hubbard, A. T.; Anson, F. C.; Gray, H. B. *J. Am. Chem. Soc.* **1967**, *89*, 3712.

(38) Ackerman, G. A.; Hesse, D. Z. *Anorg. Allg. Chem.* **1970**, *375*, 77.

(39) Lever, A. P. B. *J. Chem. Educ.* **1974**, *51*, 612.

(40) Amundsen, A. R.; Whelan, J.; Bosnich, B. *J. Am. Chem. Soc.* **1977**, *99*, 6730.

lower energy (Table IV). This would be in line with the tighter bonding expected with the hexadentate ligand, with better phenolate to iron overlap.

The tetraanionic hexadentate ligands Va and Vb, of donor atom type $O_2N_2O'_2$, form monoanionic iron complexes $[FeL]^-$ (L = Va, Vb) that absorb at 480 and 492 nm, respectively, in line with their stability constants[46] of 10^{34} and 10^{40}. Vb is less sterically constrained than Va on binding to iron, giving improved phenolate to iron overlap, thus facilitating the charge-transfer transition. The iron complexes of the hexadentate dianionic ligands VIIb and VIId, of donor atom type O_2N_4, are $[FeY]^+$ (Y = VIIb, VIId), and both carry a positive charge and have CT bands at lower energy, e.g., 507 and 509 nm, respectively, than that of the above set. This lowering in energy may be mainly attributed to the positive charge, as the CT mechanism is enhanced.

EPR Spectra and Magnetic Moments. The EPR spectra of most of the complexes show a strong signal at $g = 4.3$ and a weaker one at $g = 10$ (see Table V), typical for high-spin iron(III) in a rhombic environment, as found in the single-crystal X-ray structures of $[Fe(IIIa)_2(MeOH)_2]NO_3 \cdot MeOH$ (see earlier discussion), $Na[Fe(Va)] \cdot 4H_2O$,[34] and $[Fe(Ic)_3] \cdot 1^1/_2H_2O$.[41] The $g = 4.3$ signal is sensitive neither to the number of nitrogens or oxygens coordinated nor to the polydentate nature of the ligand. In each case there is no evidence of any splitting in the $g = 4.3$ signal as observed for Fe_2Lf and Fe_2Tf when HCO_3^- is the anion. Instead, the spectra are similar to Fe_2Tf when trinitriloacetate is the anion,[22] indicating that the precise geometry around the iron (in Fe_2Tf or Fe_2Lf) has not been achieved in these small molecule systems.

While $K[Fe(VIa)_2] \cdot 2H_2O$ and its reduced ligand form $[Fe(VIb)_2]^-$ display signals at $g = 4.3$ at −196 °C, $[Fe(VIc)_2]PF_6 \cdot H_2O$ exhibits a signal at $g = 2$ at −196 °C, indicative of a low-spin complex; however upon reduction of VIc to VId the resulting iron complex shows a high-spin signal at $g = 4.3$.

The complexes $[Fe(VIIa)]PF_6$ and $[Fe(VIIc)]PF_6$ are both low spin at −196 °C, as indicated by their $g = 2$ signals (Table V). At room temperature the former is high spin,[27] while the latter is low spin (see Experimental Section). In this case the 6,6,5,6,6-membered chelate rings of VIIc give greater stability than the 6,5,5,5,6-membered rings in VIIa. When both of these ligands are reduced, the EPR spectra of the resulting complexes show high-spin ferric iron in a tetragonal environment (Table V). $[Fe(VIII)]^+$ shows a high-spin EPR spectrum as well as its imidazole adducts (Table V). The magnetic moments for most of the complexes (see Experimental Section) are high spin at 25 °C; however for $[Fe(IV)_3] \cdot 1^1/_2H_2O$ and $[Fe(VIc)_2]PF_6 \cdot H_2O$ the values fall well short of the high-spin cases; these need further study. $[Fe(VIIc)]X$ ($X = PF_6$, I_3) are low spin.

Mössbauer Spectroscopy. Complexes of iron with Ib, Ic, and II (Table VI) have isomer shifts close to +0.5 mm/s with respect to the iron metal, indicating the ionic nature of the ligand–metal bonding in these systems, while complexes of iron with Ia, IIIa, IIIb, Va, and Vb all have isomer shifts in the range 0.37–0.41 mm/s, suggesting more covalency in their bonding and lying close to Fe_2Lf at 0.39 mm/s[45] and Fe_2Tf at 0.38 mm/s.[42]

All the complexes, including Fe_2Tf, have large quadrupole splittings, a reflection of the unsymmetric field around the ferric iron. Particularly large quadrupole splittings can be observed with $[Fe(Ib)_3] \cdot 4^1/_2H_2O$, $[Fe(IV)_3] \cdot 1^1/_2H_2O$, and $[Fe(IIIa)_2(MeOH)_2]NO_3 \cdot 2H_2O$. For the latter, the asymmetry in the ligand field has been verified by its structure (see earlier). The complexes $[Fe(Ia)_3] \cdot 6H_2O$, $[Fe(Ic)_3] \cdot 1^1/_2H_2O$, and $[Fe(II)_3]$ all show a distinct asymmetry in their absorption peaks which may be attributed either to spin–lattice relaxation effects[25] or to iron binding in two distinguishable sites in the crystal lattice.

Conclusions. The ligands used were selected to cover all types of complexes from FeO_6 to $FeO_2N_2O'_2$, and these were studied spectroscopically to determine which type or types best corresponded to Fe_2Lf. The study does show the dangers of drawing conclusions from isolated examples and difficulties in interpretation that arise when a variety of ligand systems are selected. For instance, the CT bands of the complexes involving hydroxamic acids Ia, Ib, and Ic are close in energy to Fe_2Lf and Fe_2Tf; however hydroxamato (and catecholato) ligands do not occur in Fe_2Lf, though they are found in microbial iron-transport compounds. A close fit in spectral parameters is not necessarily proof that the type and number of donor atoms are similar. From the series of complexes prepared from ligand IIIa it is evident that the energy of the charge-transfer band increases with increasing number of phenolates bound and the addition of two axial imidazoles to $[Fe(IIIa)_2(MeOH)_2]^+$ increases the CT energy relative to the parent compound. Electron buildup on the iron of the adduct (by imidazoles) increases the CT energy. A factor that decreases this energy is the increased binding strength of the ligands. Considering these factors, the high CT energy at 425 nm for the $[Fe(VIb)_2]^-$ ion (an example of an FeO_4N_2 type) would eliminate it from consideration as a model. Furthermore, the best electronic spectral fits appear to lie with the donor types FeO_3N_3 and FeO_2N_4. For these types replacement of the nitrogens present by imidazoles would be expected to raise the CT band energy even closer to that of Fe_2Lf. The extinction coefficients for these are about the same; hence they do not serve to distinguish the two. Another predictive approach can be taken. Given knowledge of the groups involved in the binding site of lactoferrin, and using $[Fe(4\text{-methylphenolato})(EtOH)_5]^{2+}$ (the tyrosyl residue is best mimicked by a para-substituted phenolate), which has a CT band in ethanol at 16 400 cm^{-1} or 610 nm,[38] as a base point, it should be possible to calculate the range of values expected for the CT band. Each bound phenolate causes a shift of about 2000 cm^{-1} toward higher energy of the CT band while each imidazole causes a shift of about 1000–2000 cm^{-1}. Thus if the binding site of Lf contains two phenolates and two imidazoles, then the CT band would be expected to be between 19 400 and 20 400 cm^{-1} or 490 and 515 nm. Ligands such as water or potentially HCO_3^- would not have a great influence on this energy. If Fe_2Lf contained three phenolates and two imidazoles, then the CT band would be between 21 400 and 22 400 cm^{-1} or 445 and 470 nm. However the tighter binding expected in Fe_2Lf might alter this range to 455–480 nm. Fe_2Lf absorbs at 465 nm (this being recorded in phosphate buffer and not ethanol), so on this basis we suggest that three and not two tyrosyl residues and two histidyl residues are likely to be bound to the ferric ion in Lf. A previous study[10] suggested that, as $Na[Fe(Va)] \cdot 4H_2O$ and Fe_2Tf had similar electronic spectral characteristics, then the latter had two tyrosyl residues bound. In light of our studies it is clear that extinction coefficient differences between FeO_2N_4 and FeO_3N_3 types are not sensitive enough for differentiation. Also the

---

(41) Linder, H. J.; Gottlicher, S. *Acta Crystallogr., Sect. B* **1969**, *B25*, 832.

(42) Spartalian, K.; Oosterhuis, W. T. *J. Chem. Phys.* **1973**, *59*, 617.

(43) Tsang, C. P.; Boyle, A. J. F.; Morgan, E. H. *Biochim. Biophys. Acta* **1975**, *386*, 32.

(44) Anderson, B. F.; Buckingham, D. A.; Robertson, G. B.; Webb, J.; Murray, K. S.; Clark, P. E. *Nature (London)* **1976**, *262*, 722.

(45) Laidriere, J.; Coussement, R.; Theuwissen, B. *J. Phys. (Paris), Colloq.* **1974**, 351.

(46) L'Eplattenier, F.; Murase, I.; Martell, A. E. *J. Am. Chem. Soc.* **1967**, *89*, 837.

correspondence in the CT transition energies may be fortuitous because (1) there are no imidazoles in ligand Va, (2) the negative charge on [Fe(Va)]$^-$ has the effect of increasing the CT energy relative to one where the charge is neutral or positive (there is no suggestion that there is a negative charge on the iron site of Fe_2Lf or Fe_2Tf), (3) a similar ligand, Vb, forms an iron complex with a lower CT energy, and if this complex had been chosen, the correspondence would have fared no better than FeO_3N_3 types, and (4) carboxylates are not thought to be bound to Fe in Lf.

The single-crystal X-ray structure of [Fe(IIIa)(MeOH)$_2$]NO_3·MeOH has shown the nitrate group not to be directly coordinated to the iron atom but interacts with it via a hydrogen-bonding system involving bound and occluded MeOH molecules. As the nitrate ion is isoelectronic and isostructural with the bicarbonate ion, which is essential for the binding iron in Fe_2Lf (and Fe_2Tf), a possibility exists that in the natural protein the bicarbonate ion may not interact directly with iron but is hydrogen bonded to a water molecule attached to it.

While many complexes have EPR spectra characteristic of Fe(III) in a rhombic environment, the $g = 4.3$ signal occupies a very narrow range of values and does not appear to be sensitive to ligand types. The unique splitting of the $g = 4.3$ signal (due to the protein conformation) for the Fe_2Lf has not been mimicked in our small molecules. Mössbauer spectroscopy is more sensitive to the ligand environment, particularly to the degree of covalent binding in the complex. The complexes [Fe(IIIa)$_3$]·1$^1/_2$$H_2O$ and Na[Fe(Va)]·4H_2O have Mössbauer parameters closest to those of Fe_2Tf, these being of the FeO_3N_3 and $FeO_2N_2O'_2$ types, respectively.

The evidence presented in this study would favor the ferric ion of Lf and Tf occupying a site of rhombic symmetry and bound to three tyrosyl and two cis histidyl residues, while the bicarbonate ion is not directly bound but is hydrogen bonded to a coordinated water molecule. A *mer*-type structure would be preferred.

Acknowledgment. We thank Dr. W. T. Robinson (University of Canterbury) for use of diffractometer facilities, Professor N. F. Curtis (Victoria University of Wellington) for use of a Faraday balance, and Dr. W. C. Tennant (Chemistry Division, DSIR) for many helpful discussions. We also thank the New Zealand University Grants Committee for financial support.

Registry No. Fe(Ia)$_3$, 14588-80-8; Fe(Ib)$_3$, 23683-82-1; Fe(Ic)$_3$, 23683-80-9; Fe(II)$_3$, 14283-77-3; Fe(IIIa)$_3$, 74877-73-9; [Fe(IIIa)$_2$(MeOH)$_2$]NO_3·MeOH, 74877-76-2; [Fe(IIIa)$_2$(MeOH)$_2$]NO_3, 74877-75-1; [Fe(IIIa)$_2$(Im)$_2$]NO_3, 74877-78-4; [Fe(IIIa)$_2$(tribenzylamine)$_2$]$^+$, 74877-79-5; [Fe(IIIa)$_2$(Me_2SO)$_2$]$^+$, 74877-69-3; [Fe(IIIa)$_2$(Me_2S)$_2$]$^+$, 74877-80-8; [Fe(IIIa)$_2$(Me_2PhPO)$_2$]$^+$, 74893-03-1; [Fe(IIIa)(MeOH)$_4$]$^{2+}$, 74877-81-9; Fe(IIIb)$_3$, 74877-82-0; Fe(IV)$_3$, 74877-83-1; Na[Fe(Va)], 16455-61-1; K[Fe(Vb)], 74877-84-2; K[Fe(VIa)$_2$], 74893-04-2; K[Fe(VIb)$_2$], 74877-85-3; [Fe(VIc)$_2$]PF_6, 74877-87-5; [Fe(VId)$_2$]PF_6, 74877-89-7; [Fe(VIIa)]PF_6, 60351-92-0; [Fe(VIIa)]NO_3, 67225-84-7; [Fe(VIIb)]PF_6, 74877-91-1; [Fe(VIIc)]PF_6, 74877-93-3; [Fe(VIIc)]I_3, 74877-94-4; [Fe(VIId)]PF_6, 74877-96-6; [Fe(VIII)]$^+$, 74877-97-7; [Fe(VIII)(Im)]$^+$, 74877-98-8; [Fe(VIII)(Im)$_2$]$^+$, 74877-99-9; [Fe(VIII)(*N*-MeIm)$_2$]$^+$, 74878-00-5.

Supplementary Material Available: A listing of observed and calculated structure factor amplitudes (9 pages). Ordering information is given on any current masthead page.

Contribution from the Istituto di Chimica Fisica,
Università di Messina, 98100 Messina, Italy

Solvent Effect on the Rates of Uncatalyzed Isomerization and Ligand Substitution at a Square-Planar Platinum(II) Complex

RAFFAELLO ROMEO,* DOMENICO MINNITI, and SANTO LANZA

Received February 13, 1980

The rates of spontaneous cis–trans isomerization of the complex *cis*-[Pt(PEt_3)$_2$(*m*-MeC_6H_4)Cl] have been measured in a variety of hydroxylic solvents and in acetonitrile. Fairly good straight lines correlate these rates and some empirical parameters which measure the relative electrophilic character of the solvent such as the α values of the Taft HDB scale or the Dimroth–Reichardt E_T values. The role of the solvent is to promote the breaking of the Pt–Cl bond in the rate-determining step, and in this respect hydrogen-bonding interactions with the leaving chloride ion are the most important factors in determining the large differences in rate observed. By way of contrast, nucleophilic displacement of the chloride ion from the same complex either by the solvent or by thiourea is little influenced by the nature of the solvent, in keeping with an associative mode of activation with a small degree of Pt–Cl bond breaking.

Introduction

Substitution reactions of 4-coordinate square-planar complexes, especially those of platinum(II), have been studied extensively, and nowadays the general mechanistic picture is reasonably clear.[1-5] The search for factors promoting the conversion of the normal associative mode of reaction into a dissociative process has then attracted much attention. It was thought to achieve this goal by one or both of the following methods: (i) prevent bond formation by using bulky ancillary ligands and/or (ii) promote bond weakening at the leaving group, usually a halide ion, by locating a strong σ donor group in trans position to it.

Increasing steric hindrance in Pd(II) and Au(III) substrates,[6] brought about by alkyl substitution on the terminal nitrogens of a coordinated ethylenetriamine ligand, leads to a large decrease of both k_1 and k_2, the nucleophile-independent and -dependent rate constants in the two-term rate law. In

---

(1) Basolo, F.; Pearson, R. G. "Mechanisms of Inorganic Reactions", 2nd ed.; Wiley: New York, 1967; Chapter 5.

(2) Langford, C. H.; Gray, H. B. "Ligand Substitution Processes"; Benjamin: New York, 1966; Chapter 2.

(3) Tobe, M. L. "Inorganic Reaction Mechanisms"; Nelson: London, 1972; Chapter 5.

(4) (a) Cattalini, L. *Prog. Inorg. Chem.* **1970**, *13*, 263. (b) Cattalini, L. *MTP Int. Rev. Sci.: Inorg. Chem., Ser. One* **1972**, *9*, Chapter 7.

(5) Wilkins, R. G. "The Study of Kinetics and Mechanisms of Reactions of Transition Metal Complexes"; Allyn and Bacon: Boston, 1974; Chapter 4.

(6) (a) Reference 3, p 64. (b) Fant, D. L.; Weick, C. F. *Inorg. Chem.* **1973**, *12*, 1864.

0020-1669/80/1319-3663$01.00/0 © 1980 American Chemical Society